# Supersonic Boundary-Layer Stability Analysis on an Aircraft Wing

Shreekant Agrawal* and Thomas A. Kinard†
*McDonnell Aircraft Company, McDonnell Douglas Corporation, St. Louis, Missouri 63166*
and
Arthur G. Powell‡
*Douglas Aircraft Company, McDonnell Douglas Corporation, Long Beach, California 90846*

**An analysis of the boundary layer and its stability with and without suction on a supersonic cruise fighter wing configuration is presented for a freestream Mach number of 2.0 and an angle of attack of 4.0 deg. The inviscid pressures obtained from an Euler solver are used to generate the boundary-layer solutions using an improved version of the method of Kaups and Cebeci. The boundary-layer stability is analyzed with the linear theory for compressible flow. The well-known $e^n$ method, with an $n$ value of 9, is used to predict transition. The largest amplifications are found for highly oblique traveling crossflow (CF) type waves, oriented at approximately 80 deg without suction and 87.5 deg with suction, measured from the local external velocity vector. These oblique traveling CF waves are found to exhibit much larger growth than stationary crossflow waves when suction is not applied. A level of suction is determined that contains the growth of these waves to amplification factors less than 9, delaying predicted transition to the target chord location of 60%.**

## Nomenclature

| | |
|---|---|
| $A$ | = disturbance amplitude at any point |
| $A_0$ | = disturbance amplitude at the neutral stability point |
| $C,c$ | = chord length, ft |
| $CFX$ | = local skin-friction coefficient based on components in the negative $x$-coordinate direction |
| $CFZ$ | = local skin-friction coefficient based on components in the $\theta$-coordinate direction |
| $Cp$ | = pressure coefficient, $2(p/p_\infty - 1)/(\gamma M_\infty^2)$ |
| $Cp''$ | = second derivative of pressure with respect to $\bar{x}/c$ |
| $CQ$ | = suction coefficient, $\rho_w v_w/\rho_\infty V_\infty$ |
| $DELSTX$ | = boundary-layer displacement thickness based on $U_e$ |
| $DELSTZ$ | = boundary-layer displacement thickness based on $W_e$ |
| $DELTA$ | = boundary-layer thickness |
| $DELTCF$ | = $\int_0^{Y_{0.95}} v_\ell \, dy/V_e$ |
| $F$ | = disturbance frequency, Hz |
| $M_\infty$ | = freestream Mach number |
| $N,n$ | = amplification factor, $\ell n(A/A_0)$ |
| $p$ | = static pressure |
| $p_\infty$ | = freestream pressure |
| $Psi$ | = wave orientation angle with respect to the local external flow velocity vector, deg |
| $R_e$ | = Reynolds number, $V_e x/\nu_e$, based on $x$ |
| $R_\theta$ | = Reynolds number, based on momentum thickness |
| $R_{\theta\, n=9}$ | = Reynolds number corresponding to $n$ factor equal to 9 |
| $U, u$ | = velocity component in $x$-coordinate (radial) direction |
| $V$ | = local resultant velocity |
| $W, w$ | = velocity component in $\theta$-coordinate (circumferential) direction |
| $x,\theta,y$ | = polar coordinate system in the developed plane of the wing surface |
| $\bar{x}, \bar{y}, \bar{z}$ | = Cartesian coordinate system used for wing definition: $\bar{x}$ is chordwise and $\bar{y}$ is spanwise; $\bar{z} = 0$ is the wing chord plane |
| $XLENC$ | = wavelength-to-chord ratio |
| $Y$ | = distance normal to the surface |
| $Y_{0.95}$ | = distance normal to the surface corresponding to the point where local velocity = 0.95 × $V_e$ |
| $\alpha$ | = angle of attack, deg |
| $\gamma$ | = ratio of specific heats, = 1.4 |
| $\theta$ | = polar coordinate in the developed plane, also momentum thickness |
| $\lambda_1$ | = leading-edge sweep of the wing |
| $\lambda_2$ | = trailing-edge sweep of the wing |
| $\nu$ | = local kinematic viscosity |

*Subscripts*

| | |
|---|---|
| $\infty$ | = freestream condition |
| $e$ | = local external flow condition |
| $w$ | = wall condition |

Received May 12, 1990; revision received Nov. 15, 1990; accepted for publication Dec. 1, 1990. 

*Technical Specialist, Aerodynamics, CFD Project. Associate Fellow AIAA.
†Senior Engineer, Aerodynamics, CFD Project. Member AIAA.
‡Principal Engineer/Scientist, Aerodynamics Technology. Member AIAA.

## Introduction

In recent years, viscous flow drag reduction technology has advanced rapidly. Progress in laminar flow control (LFC) technology in the past 10 years has shown that laminar flow over large areas of aircraft wing and empennage surfaces is not only feasible but also practical for many full-scale subsonic and transonic applications.[1] The same cannot be said, however, for supersonic flows, since insufficient research has been conducted in this flow regime to date. The greater sweep angles and lower aspect ratios, etc., make the integration of LFC technology into the design a very challenging task. Preliminary studies indicate the potential for sizing benefits on military fighters if laminar boundary-layer flow can be attained in the low supersonic flight regime ($M_\infty$ = 1.0–2.5). The development of supersonic LFC capabilities, therefore, appears to be an area for technological advancement.

The boundary-layer flow over a swept wing is highly three dimensional. Many mechanisms exist that can cause boundary-layer transition. The first category is what Morkovin calls

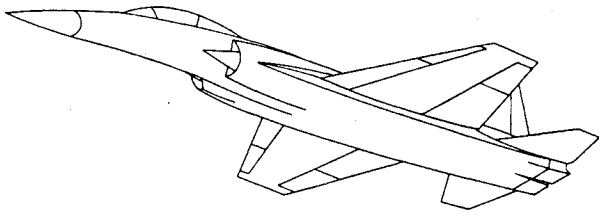

**Fig. 1 SF-1107 multirole supersonic fighter configuration.**

the "bypass mechanisms."[2] Freestream turbulence, fuselage turbulence propagated along the attachment line, noise, separation, surface waviness, roughness (bugs, ice), etc., are included in this category. Their absence or minimum influence is a prerequisite for laminar flow to exist. Other mechanisms include the Tollmien-Schlichting (T-S), crossflow (CF), and the Göertler instabilities.[3]

Along the attachment line of a swept wing, where the normal flow stagnates, a spanwise flow boundary layer exists. The stability of this boundary layer is of obvious importance to the flow over a wing. T-S instability can exist in the flow along the attachment line and elsewhere, even in the absence of pressure gradients. This instability is associated with viscous effects and is very sensitive to the shape of the velocity profiles, with robust profiles being more stable. Boundary-layer crossflow occurs in regions of both adverse and favorable pressure gradients on a swept wing. The crossflow velocity profiles are highly inflectional. They are known to be unstable, giving rise to nearly streamwise corotating boundary-layer vortices known as crossflow waves. Göertler instability arises in laminar boundary layers over concave walls and is due to centrifugal forces. It is not a concern in predominantly convex geometries. These different types of instabilities must be considered before any conclusions can be drawn about transition.

Current methods for boundary-layer stability analyses are based on linear theory. Such a theory provides boundary-layer disturbance amplitudes relative to their values at the neutral stability point. The natural logarithm of this ratio is called the amplification factor, or $n$ factor. When this quantity reaches a value on the order of 9–11, transition can be expected to occur.[4] This method of determining transition is commonly called the $e^n$ method and has been found to work well for a variety of subsonic, transonic, and supersonic flows. In the present analysis, an $n$ value of 9 is used as the transition criterion.

Our analysis of the boundary layer and its stability with and without suction is based on a supersonic cruise fighter wing configuration. The overall procedure is similar to that in Ref. 5. It consists of first determining the inviscid pressures on the surface of the wing using the FLO67 Euler code.[6] The boundary-layer solutions corresponding to these pressures are then determined using the Kaups-Cebeci method[7] and subsequently analyzed using the COSAL code,[8] based on linear stability theory. The suction distribution is determined by an iterative process.

The Kaups-Cebeci (K-C) code has proven very effective in those transonic applications where a conical pressure field exists.[9-11] Its application to supersonic Mach numbers presents new challenges. Higher Mach numbers and sharper leading edges, for example, result in much larger variations in boundary-layer thickness than those encountered in transonic applications. Also, the assumption of isentropic flow external to the boundary layer is invalid when significant entropy variations occur across any shock waves. Therefore, the input to the K-C code was modified to include the effects of entropy variations in the flow external to the boundary layer, and modifications were made to the code to ensure an adequate number of points in the boundary layer at all stations. The modified code provided better resolution of the boundary layer for cases having supersonic freestreams and sharp leading edges.

The complete configuration under study is shown in Fig. 1; however, only the wing geometry was analyzed. All the results shown are for a freestream Mach number of 2.0, a cruise angle of attack of 4.0 deg, and a standard day altitude of 40,000 ft.

## Results

### Inviscid Flow Solutions

The inviscid flow solutions on the isolated wing were obtained using the FLO67 Euler code. The wing consisted of parabolic biconvex airfoils of 5% thickness. Wing chord ranged from 22.50 ft at the centerline to 5.45 ft at the tip. The pressure distributions were found to be very smooth, an essential condition for accurate stability analysis. The surface pressure distribution at 50% semispan station is shown in Fig.

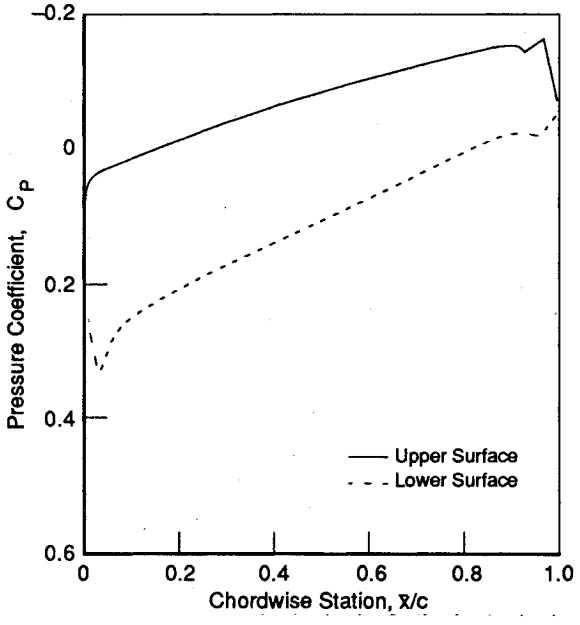


**Fig. 2 Pressure distribution at 50% semispan, $M_\infty = 2.0$, $\alpha = 4$ deg.**

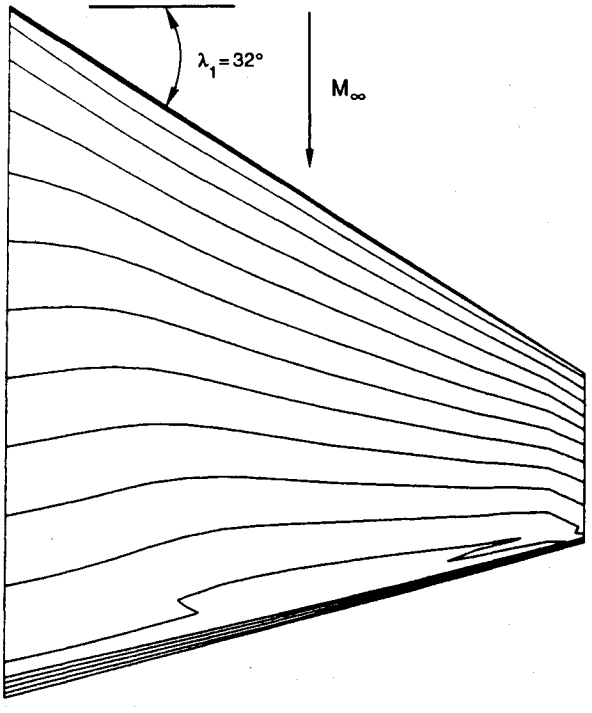


**Fig. 3 Upper surface pressure contours, $M_\infty = 2.0$, $\alpha = 4$ deg.**

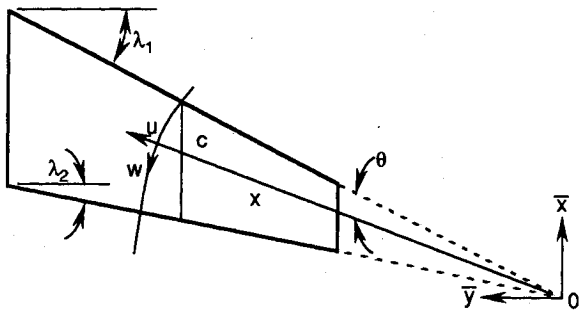


Fig. 4 Tapered wing and conical coordinate system.

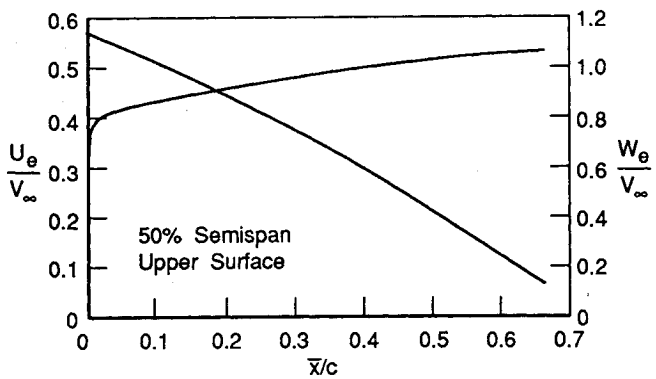


Fig. 5 External velocity components in the radial and circumferential directions, $M_\infty = 2.0$, $\alpha = 4$ deg.

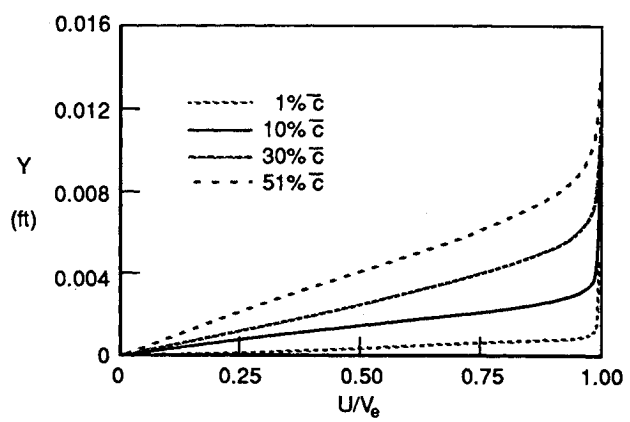


Fig. 6 Radial velocity profiles at different chord stations, 50% semispan.

2. The corresponding upper surface pressure contours, which were also very smooth, are shown in Fig. 3.

Such airfoils produce favorable chordwise pressure gradients. Although this favorable gradient controls the growth of T-S waves, on a swept wing it can amplify crossflow growth.

### Boundary-Layer Analysis Without Suction

An accurate stability analysis requires accurate calculation of mean velocity profiles of the boundary layer. The K-C code is based on a conical flow assumption (i.e., pressure isobars along constant percent chord lines or along the generators if the wing has a trapezoidal planform). The coordinate system used by the program is shown in Fig. 4. Since such straight isobars are generally not achievable near the wing root and the wing tip, the method at first may not appear to be very suitable for low aspect ratio wings. However, as can be seen from Fig. 3, highly conical isobars on the upper surface of the wing are found with the biconvex section. The assumption of conical flow as used in the K-C code is, therefore, not violated for the case under consideration.

The boundary-layer solutions for supersonic flows obtained using the modified version of the K-C code were then examined in detail to increase confidence in their stability characteristics. Some sample results of the analysis are shown in Figs. 5–7. Those results shown here are for 50% semispan on the upper surface without using any boundary-layer suction.

Figure 5 shows very smooth distributions of velocities $U_e$ and $W_e$, obtained from the FLO67 Euler code, in the polar coordinate system (Fig. 4) as used in the K-C code. Those distributions are plotted against the chord stations $\bar{x}/c$. The smooth distributions are necessary for accurate stability calculations.

The boundary-layer velocity profiles along the radial direction are shown in Fig. 6 at four different locations ranging from 1 to 51% chord stations. Figure 7 shows the high degree of self-similarity of typical consecutive velocity profiles in scaled coordinates *Y/DELSTX*. Although not demonstrated through this figure, a closer examination indicates that these profiles do not indeed fall on a single curve as anticipated for nonzero pressure gradients. An accurate stability analysis also depends on how accurately the second derivative of velocity with respect to the coordinate normal to the wing is calculated. Such a derivative must be free of numerical oscillations, which was the case in this study.

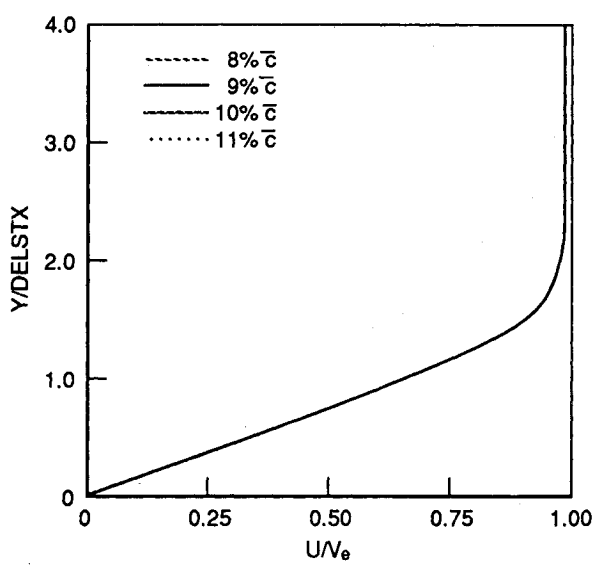


Fig. 7 Radial velocity profiles at four consecutive chord stations, 50% semispan.

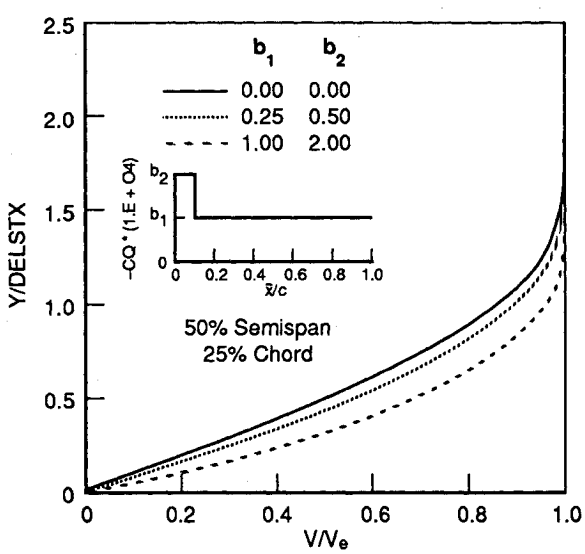


Fig. 8 Effect of suction on velocity profiles.

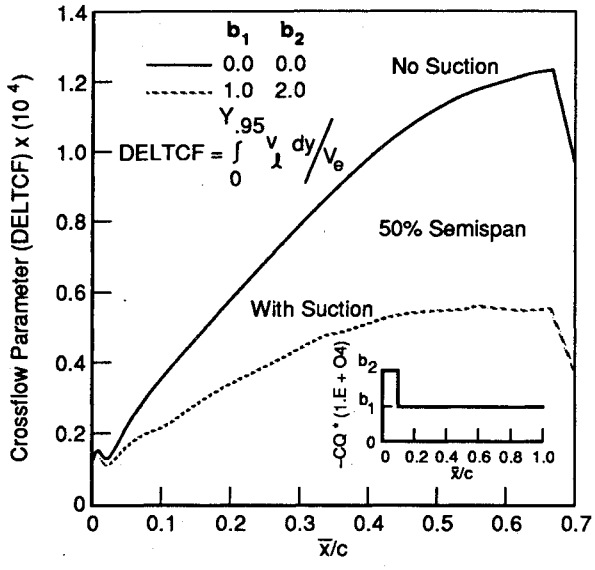


Fig. 9 Effect of suction on a crossflow parameter.

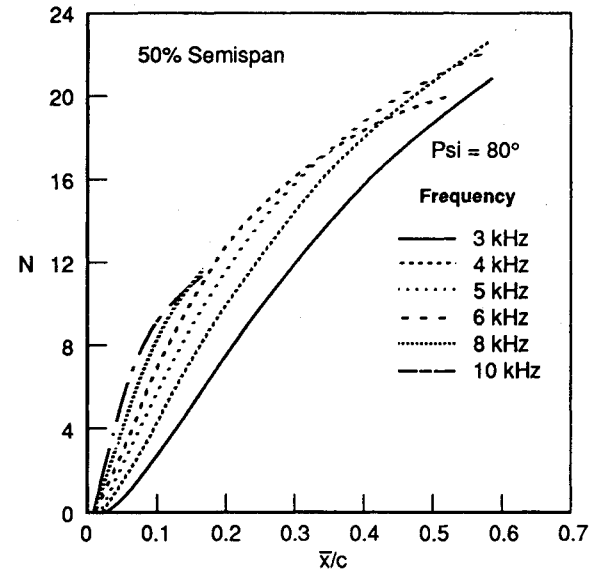


Fig. 12 Amplification factor for different frequencies, no suction.

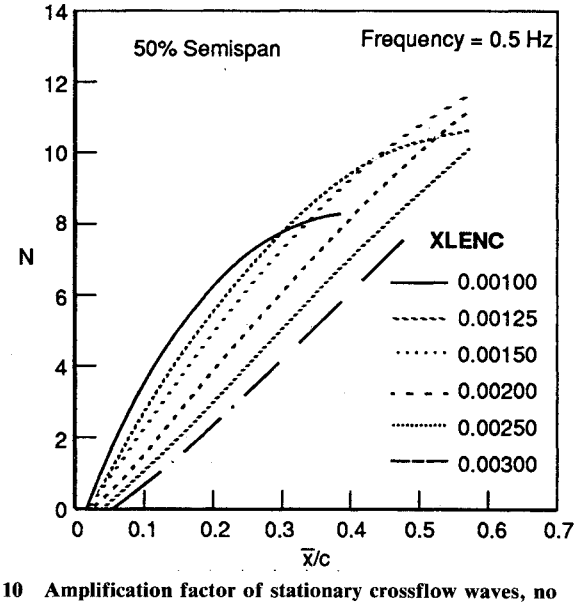


Fig. 10 Amplification factor of stationary crossflow waves, no suction.

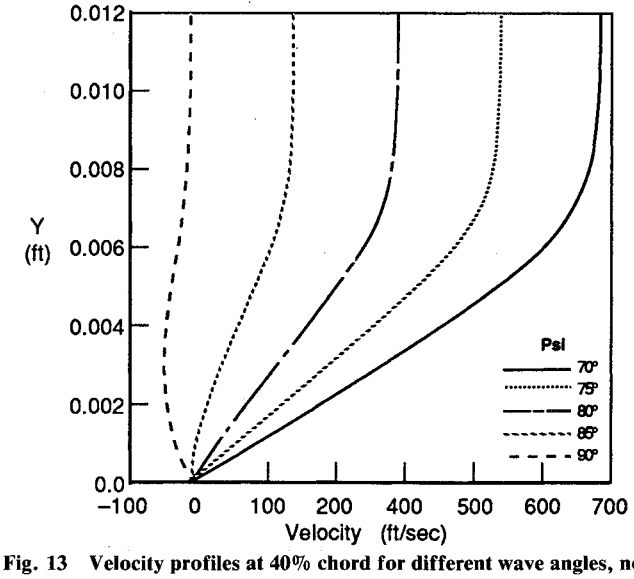


Fig. 13 Velocity profiles at 40% chord for different wave angles, no suction, 50% semispan.

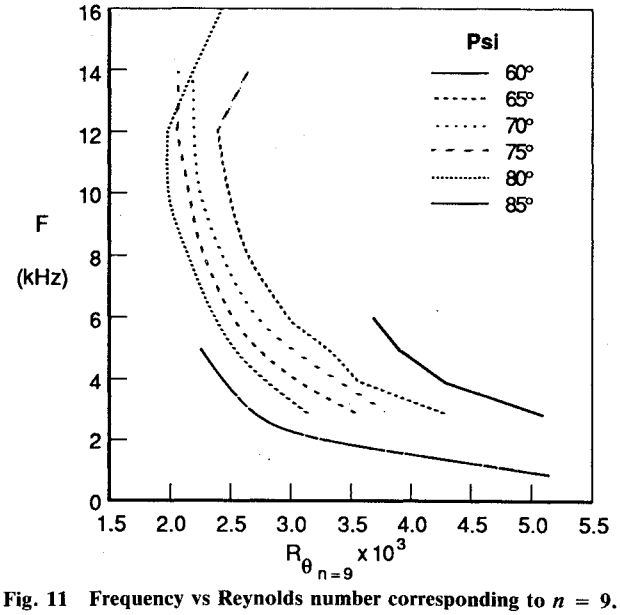


Fig. 11 Frequency vs Reynolds number corresponding to $n = 9$.

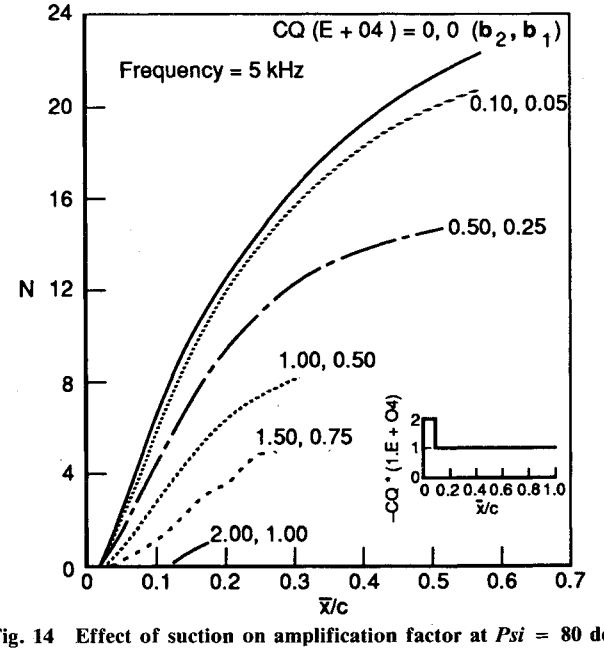


Fig. 14 Effect of suction on amplification factor at *Psi* = 80 deg, 50% semispan.

### Boundary-Layer Analysis with Suction

Before conducting stability analysis, the effects of suction on the boundary layer were also studied. There are several effects of suction. Suction thins the boundary layer and thereby lowers the effective Reynolds number. This effect is demonstrated in Fig. 8 where the boundary-layer velocity profiles at 25% chord station are plotted against the normal coordinate $Y$ for different suction values $CQ$. With increased suction, the thickness of the boundary layer is reduced considerably. Another effect of suction is to change the boundary-layer shape factor. This is quite evident from Fig. 8, which shows that the profile shape also changes appreciably.

The suction also causes the inflection point of the CF profile to move closer to the wall where the increased viscosity acts to stabilize the crossflow instability. This is demonstrated in Fig. 9, where a CF parameter (*DELTCF*) is plotted against the chord stations for different suction levels. This CF parameter is an integrated value of the CF boundary-layer thickness. It is quite clear that this thickness is reduced substantially with suction. All these effects of suction are known to have stabilizing influence on the boundary-layer stability.[12]

### Stability Analysis Without Suction

Stability analysis of the boundary-layer profiles obtained from the K-C code was performed using COSAL. Analysis with and without suction was conducted to determine the most amplified disturbance. In this study, both the constant wave angle and constant wavelength options were used. Growth of stationary and nonstationary crossflow waves was calculated. Both upper and lower surfaces of the wing were examined in detail. Three spanwise stations (inboard, midspan, and outboard) were analyzed.

Initially, a broad range of frequencies, wave angles, and wavelengths were analyzed to identify the most amplified dis-

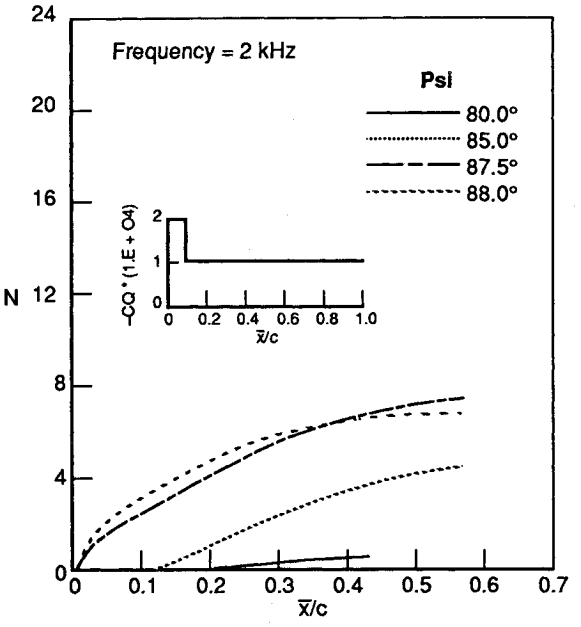


Fig. 15 Amplification factor for different wave angles, with suction, 50% semispan.

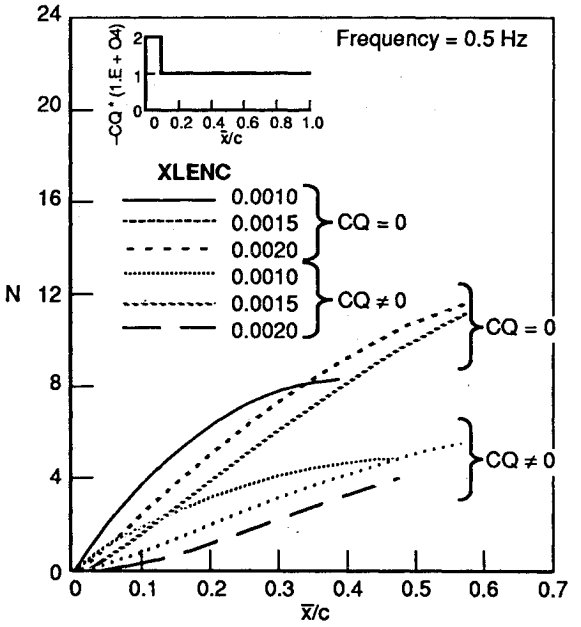


Fig. 16 Effect of suction on the growth of stationary crossflow waves, 50% semispan.

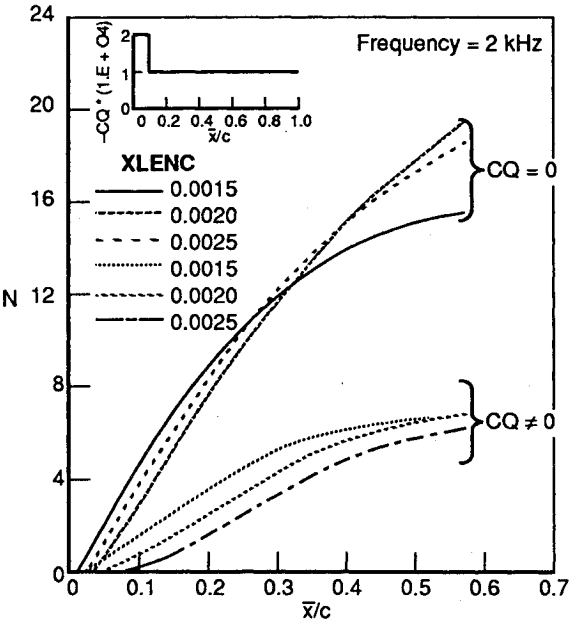


Fig. 17 Effect of suction on the growth of nonstationary crossflow waves, 50% semispan.

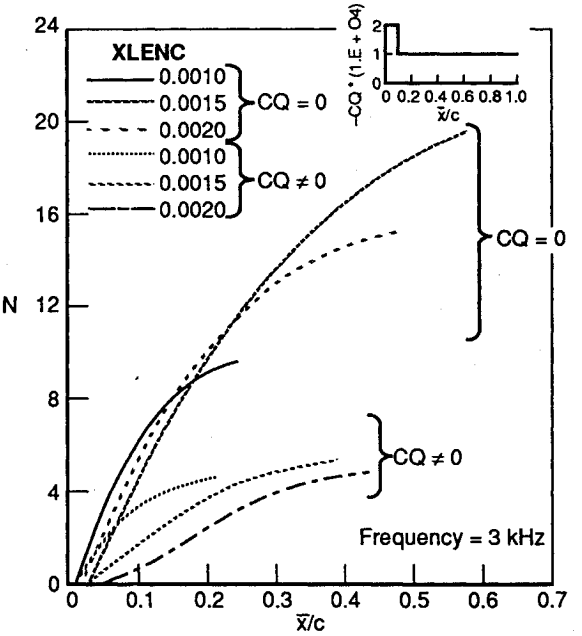


Fig. 18 Effect of suction on the growth of nonstationary crossflow waves, 50% semispan.

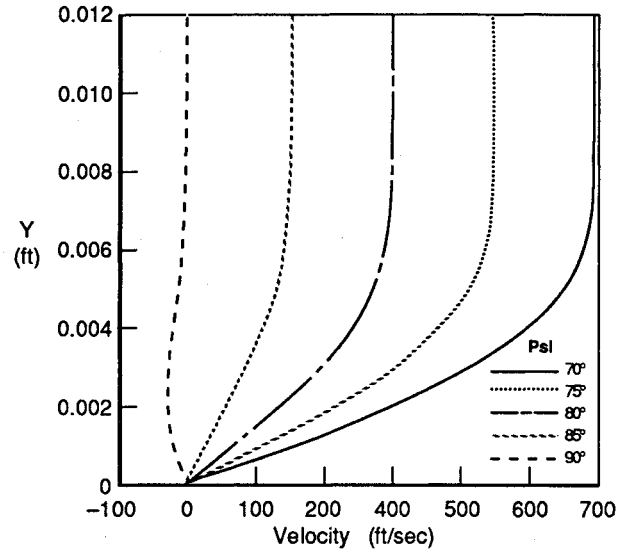


**Fig. 19 Velocity profiles at 40% chord for different wave angles, with suction, 50% semispan.**

turbances. Figure 10 shows the results of stationary ($F$ = 0.5 Hz) CF stability analysis without suction. The $n$ factors are plotted against $\bar{x}/c$ for different values of the wavelength-to-chord ratio (*XLENC*, CF vortex spacing). An attempt was made to find a band of *XLENC* for which the growth of these instabilities could be important, and it appears that the band lies between 0.0010 and 0.0030. The maximum amplification occurs near *XLENC* = 0.0015.

Figure 11 shows the stability calculations without suction, where frequency is plotted against $R_{\theta n=9}$ for several different wave orientation angles. Here $R_{\theta n=9}$ is defined as the momentum thickness Reynolds number corresponding to the first occurrence of the $n$ factor of 9. Since the $n$ factor changes with wavelength, wave angle, and frequency, $R_{\theta n=9}$ as defined here is a variable. It is observed that the minimum $R_{\theta n=9}$ is approximately 1935 (~ at 8% chord station), and the frequency and the orientation angle of the corresponding wave are 10–12 kHz and 80 deg, respectively. The largest $n$ factors computed are found for frequencies around 5 kHz and *Psi* = 80 deg. The corresponding value of *XLENC* was found to be around 0.0040 (not shown here). Figure 12 shows the $n$ factors for *Psi* = 80 deg and several different frequencies. The $n$ factor first reaches a value of 9 at approximately 8% chord location for $F$ = 10 kHz. This indicates that natural laminar flow would exist only up to 8% chord location. For a frequency value of 5 kHz, the $n$ factor reaches a value as high as 23, whereas for higher frequencies, these values are considerably smaller. The high-frequency waves have a quicker growth but become stable in a short distance from the leading edge due to a thickening downstream boundary layer.

It is worth noting here that the linear stability theory may not be quite valid when the $n$ factors are above a value of about 12.[4] However, such high values of $n$ factors calculated from linear theories should not be discarded. They should be used as indications of the possible instability that may exist for that particular combination of frequency, wavelength, and wave angle.

The boundary-layer velocity profiles on the wing were analyzed to gain insights into the type of instabilities present at high wave angles as observed here. The velocity profiles resolved along different wave orientation angles were examined at several chord stations at the 50% semispan location. The analysis offered some valuable information about the development of inflections in the velocity profiles from leading edge to the 60% chord location, target region for laminar flow, for different wave orientation angles. These results are shown in Fig. 13. It is observed that at *Psi* = 70 deg, inflection is almost absent, whereas above *Psi* = 70 deg, e.g., at 80 deg, there is clear evidence of inflection that becomes even stronger at 85 deg. The crossflow profiles corresponding to *Psi* = 90 deg are also shown in the figure.

This analysis does indicate that the highly oblique waves (above approximately *Psi* = 80 deg) as determined from the stability results are indeed crossflow waves, which are due to inflectional velocity profiles.

#### Stability Analysis with Suction

The boundary-layer stability with suction has also been analyzed in detail. The next several figures show the stability calculations with suction. Figure 14 shows the effect of suction on the amplification factor for *Psi* = 80 deg and $F$ = 5 kHz. With progressively increasing suction, growth of the waves can be almost eliminated.

Since the aim should be to apply just enough suction so that the $n$ factors do not grow beyond a value of 9 (assuming that this number is the limit above which laminar flow cannot be maintained), the boundary layer should not be oversucked since that has several adverse effects, e.g., larger perturbations caused by the suction holes, increased weight of the suction systems, and increased skin friction, etc. From this figure, it might appear that the suction level corresponding to label (1.00, 0.50), which is shown in the same figure in the lower right-hand corner, is perhaps sufficient. However, further stability calculations indicated that a higher level of suction was needed, labeled as (2.00, 1.00) in the same figure. This distribution was used in several calculations to make sure that the growth of neither stationary nor nonstationary CF instabilities ever reached a value of 9. Some of these results are shown in Figs. 15–18.

One effect of applying suction was a much greater damping of the high-frequency waves. For example, compare the effect of applying suction, labeled as (2.00, 1.00), on waves of frequency 5 kHz (Fig. 14) with the same at 2 kHz (Fig. 17). This results in a shift of the most amplified wave to a lower frequency (from 5 to 2 kHz) when suction, labeled as (2.00, 1.00), was applied.

Figure 15 shows the amplification factors for several different values of *Psi*, but fixed at a constant frequency of 2 kHz. Calculations are shown here for $F$ = 2 kHz only, since it corresponds to the most amplified disturbance. The distribution of suction level is also shown in the figure. Once again it is noticed that the largest amplification is found to be for highly oblique waves (87.5 deg in this case). In fact, the orientation angle of the most amplified wave has increased as a result of suction application. Stationary CF calculations are shown in Fig. 16, whereas nonstationary CF calculations for $F$ = 2 and 3 kHz are shown in Figs. 17 and 18. The value of *XLENC* corresponding to the most amplified disturbance is found to be about 0.0020 (Fig. 17). It is worth noting that the effect of suction on the amplification of nonstationary CF instabilities is much larger than that on the stationary CF instabilities (Figs. 16–18).

An analysis, similar to that shown in Fig. 13, was also conducted to examine the development of inflections in the boundary-layer velocity profiles with suction. The semispan and chord locations were the same as in Fig. 13. The results from this analysis are shown in Fig. 19. Not surprisingly, the profile shapes change considerably when suction is applied. The boundary layers are thinner, as expected. Moreover, the inflections are almost absent at *Psi* = 80 deg. However, they do show their presence at 85 deg and beyond. Once again, this analysis indicates that the highly oblique waves (*Psi* = 87.5 deg) corresponding to the largest amplification factor as determined from the stability results are indeed traveling crossflow waves. The effect of suction, therefore, is to move the visible inflection to a higher wave angle.

Similar results have also been obtained at 18.75 and 81.25% semispan locations on the SF-1107 wing. Since the pressure distributions at these locations are very similar to those at 50% location, calculations were minimized considerably. Knowing

the trends of the different instability growths at 50% semispan, the ranges of frequencies, wavelengths, and wave orientation angles were bracketed very well. Results for those calculations are not shown here since they were very similar to those at 50% semispan.

Calculations were also performed on the lower surface at the same three span stations. Without suction, the transition is predicted to occur very close to the leading edge. This can be expected since an adverse pressure gradient exists near the leading edge of the wing for the conditions examined (Fig. 2). With suction (distribution shown in Fig. 14), the predicted location of transition was delayed to 60% chord. If a less favorable pressure gradient had been used, then less suction would have been required.

#### Attachment Line and Göertler Instability Considerations

The SF-1107 wing consists of parabolic biconvex airfoil of 5% thickness; therefore, the geometry is predominantly convex. Hence, Göertler instabilities would not be expected to present problems for this configuration.

The attachment line instability was analyzed using the criterion of momentum thickness Reynolds number ($R_\theta$). This criterion is from Bacon and Pfenninger.[13] The attachment line laminar boundary layer is stable, and any large disturbances will damp out if $R_\theta < 100$. For $100 < R_\theta < 240$, it is stable to small disturbances, and large disturbances, such as turbulence, will persist. For $R_\theta > 240$, however, the attachment line boundary layer is unstable to small disturbances, and transition occurs spontaneously. For the SF-1107 wing, the values of $R_\theta$ with suction were found to be 46.06, 38.74, and 30.51 at 18.75, 50, and 81.25% semispan locations, respectively. Therefore, the attachment line instability is not expected to pose any difficulty.

## Concluding Remarks

An analysis of the boundary layer and its stability with and without suction on a supersonic cruise fighter wing having biconvex 5% thick airfoils is conducted for a freestream Mach number of 2.0 and an angle of attack of 4.0 deg. It is found that the largest amplification is due to the highly oblique traveling crossflow-type waves, oriented approximately 80 deg without suction and 87.5 deg with suction from the local external velocity vector. It is concluded that with the biconvex airfoil section on the thin swept wing, this type of instability would be the likely cause of transition.

The approximate values of frequency, wave orientation angle, and wavelength-to-chord ratio for the most amplified disturbance for the no-suction case are found to be 5 kHz, 80 deg, and 0.0040, respectively. However, transition would be expected to occur as a result of waves at 10–12 kHz at 80 deg, which grow more quickly to the critical $n$ factor of 9. When suction is applied, the most amplified waves are found at approximately 2 kHz, 87.5 deg, and 0.0020, respectively.

With no suction, growth of the stationary CF is much smaller than the traveling CF-type instabilities. Growth of the instabilities have been demonstrated to be reduced significantly with suction. The effect of suction on the nonstationary CF instabilities is much larger than that on the stationary CF instabilities. The effect of suction was seen as an increase in the wave angle and a corresponding decrease in the frequency of the most amplified wave. A low level of suction ($CQ = 0.0002$ for $0 \le \bar{x}/c \le 0.1$, and $CQ = 0.0001$ for $\bar{x}/c > 0.1$) was sufficient to prevent the growth of these instabilities from reaching an $n$ factor of 9. The transition location, based on the $e^9$ method, was delayed from approximately 8% chord on the upper surface, and less than 1% on the lower surface, to the target chord location of 60%. The attachment line and Göertler instabilities are not expected to present any difficulty for such wings.

## Acknowledgments

The present study was conducted under NASA Contract NAS1-18037. Dal V. Maddalon of the NASA Langley Research Center was the contract monitor. Many valuable suggestions made by him and his colleagues, during the preparation of the manuscript, are greatly appreciated. Also, the authors acknowledge the valuable assistance of Alan Cain of McDonnell Douglas Corporation.

## References

[1]Anon., "Research in Natural Laminar Flow and Laminar Flow Control," NASA-CP-2487, March 1987.

[2]Morkovin, M. V., "Instability, Transition to Turbulence and Predictability," AGARDograph No. 236, July 1978.

[3]Saric, W. S., and Reed, H. L., "Three-Dimensional Stability of Boundary Layers," *Perspectives in Turbulence Studies: Proceedings of the International Symposium,* Springer-Verlag, Berlin, May 1987, pp. 71–92.

[4]Hefner, J. N., and Bushnell, D. M., "Status of Linear Boundary Layer Stability Theory and the $e^n$ Method, with Emphasis on Swept-Wing Applications," NASA TP-1645, April 1980.

[5]Pfenninger, W., and Vemuru, C. S., "High Subsonic Speed LFC Transport Airplanes: Boundary Layer Crossflow Stabilization, Wing Analysis and Design," AIAA Paper 88-0275, Jan. 1988.

[6]Jameson, A., "A Vertex Based Multigrid Algorithm for Three-Dimensional Compressible Flow Calculations," *Numerical Methods for Compressible Flows—Finite Difference, Elements, and Volume Techniques,* ASME-AMD-Vol. 78, American Society of Mechanical Engineers, New York, Dec. 1986, pp. 45–73.

[7]Kaups, K., and Cebeci, T., "Compressible Laminar Boundary Layers with Suction on Swept and Tapered Wings," *Journal of Aircraft,* Vol. 14, No. 7, July 1977, pp. 661–667.

[8]Malik, M. R., "COSAL—A Black Box Compressible Stability Analysis Code for Transition Prediction in Three-Dimensional Boundary Layers," NASA CR-165925, May 1982.

[9]Srokowski, A. J., and Orszag, S. A., "Mass Flow Requirements for LFC Wing Design," AIAA Paper 77-1222, Aug. 1977.

[10]Dagenhart, J. R., "Amplified Crossflow Disturbances in the Laminar Boundary Layer on Swept Wings with Suction," NASA TP-1902, Nov. 1981.

[11]Anon., "Final Report—Laminar Flow Control Leading Edge Glove Flight Test Article Development," NASA CR-172137, Nov. 1984.

[12]Lekoudis, S. G., "Stability of Three-Dimensional Compressible Boundary Layers over Wings with Suction," AIAA Paper 79-0265, Jan. 1979.

[13]Bacon, J. W., Jr., and Pfenninger, W., "Transition Experiments at the Front Attachment Line of a 45 Degree Swept Wing with a Blunt Leading Edge," Air Force Flight Dynamics Lab., AFFDL TR-67-33, Wright-Patterson AFB, OH, June 1967.